Journal of Materials Chemistry A

COMMUNICATION

Supplementary Information

Sulfur and Nitrogen Co-Doped Holey Graphene Aerogel for Structurally Resilient Solid-State Supercapacitors under High-Compressions

Moumita Kotal,[a] Hyunjun Kim,[a] Sandipan Roy [a] and Il-Kwon Oh* [a]

[a] Creative Research Initiative Center for Functionally Antagonistic Nano-Engineering,Department of Mechanical Engineering, School of Mechanical and Aerospace Engineering,Korea Advanced Institute of Science and Technology (KAIST),291 Daehak-ro, Yuseong-gu, Daejeon 34141, Republic of Korea. *E-mail : ikoh@kaist.ac.kr

Experimental section

Chemicals

All checmicals were received from commercial sources and used without further purification. Natural graphite powder (Samjung C & G Co. Ltd.), $NaNO_3$ (Sigma-Aldrich), $KMnO_4$ (Sigma-Aldrich), 98% $H2SO_4$ (Daejung Chemical Industry Co. Ltd.), 30% H_2O_2 solution (Sigma-Aldrich), Cysteamine (Sigma- Aldrich), Poly (vinyl alcohol) (Sigma-Aldrich) and LiCl (Sigma-Aldrich) were used as received.

Preparation of N and S co-doped holey graphene aerogel (NS-HGA)

NS-HGA was produced by three steps; oxidative etching of carbon atoms, hydrothermal assisted synthesis and thermal annealing. Briefly, GO was prepared by oxidation of natural graphite powder using modified Hummers method.[1] A controlled amount of H2O2 aqueous solution (3 mL 0.3% H2O2) with GO aqueous dispersion (25 mL, 5 mg mL^{-1}) was refluxed for 3h to prepare nanopores with oxygen containing groups at the defective sites on the basal plane of graphene oxide. After that, cysteamine-functionalized holey graphene oxide was prepared using hydrothermal method by keeping the solution of holey graphene oxide with cysteamine (160 mg) in a 50 mL Teflon-lined autoclave under 180 °C for 10 h followed by cooling down to room temperature. The as-prepared cysteamine bridged holey graphene hydrogel was dialyzed by water for 24h to remove the residual impurities, and then subjected to prefrozen (-10 °c) for 12h to create the additional pores using the ice templates followed by lyophilizing (at -50 °C for 1.5 d) to form aerogel. Finally, to improve the electrical conductivity as well as N and S co-doping level, it was annealed at 800 °C for 2 h under Ar atmosphere to prepare NS-HGA.

Preparation of N and S co-doped graphene aerogel (NS-GA) and pristine graphene aerogel

NS-GA was prepared by adding cysteamine (160 mg) to GO aqueous dispersion (25 mL, 5 mg mL^{-1}) in a 50 mL Teflon-lined autoclave under 180 °C for 10 h followed by same procedure used for NS-HGA. Pristine graphene aerogel was prepared using the same procedure without adding cysteamine.

Fabrication of structurally resilient solid-state supercapacitors (SRSS)

Two-types of structurally resilient solid-state supercapacitor devices were assembled; one was the cutting of ~2 mm thickness of individual NS-HGA, NS-GA followed by pressing to make flat thin electrode (1.2×0.96 cm^2), while the other one was the cutting of cubic shaped NS-HGA aerogel (0.8×0.8 cm^2). The gel electrolyte was prepared by mixing 8.5 g LiCl and 4 g PVA in 40 mL deionized water under vigorous stirring at 85 °C for 2h followed by cooling down. Typically, the two pieces of both NS-GA and NS-HGA flat thin electrodes connected to Cu foil by silver paste were immersed in the gel electrolyte for 5 min then assembled together using ion-porous separator (Celgard 3401) soaked with gel electrolyte. The device was kept at 45 °C for 12 h to remove excess water in the electrolyte to provide total thickness of 0.0425 cm. Hence, the whole area of two electrodes was about 2.3 cm^2, while total volume of the device was about 0.05 cm3. On the contrary, in case of cubic-shaped NS-HGA, compressible SRSSs were assembled by connecting the two pieces of cubic-shaped NS-HGA (0.8×0.8 cm^2) through Cu foil by silver paste followed by dropping PVA/LiCl gel electrolyte onto the surfaces of the electrodes till NS-HGA cube was saturated. Then all parts were assembled together with one piece of Celgard 3401 separator soaked with gel-electrolyte. Finally, compressible ASSC was kept at 45 °C for 12 h to remove the excess water from the electrolyte to form the total height of the device about 2.2 cm and thereby total volume of the device of about 1.41 cm^3 (or total area of two electrodes ~ 1.28 cm^2).

Materials Characterization

The morphologies and structures of all of the samples were characterized by FESEM (Magellan 400 FEI at 1 kV), HRTEM (Titan cubed G2 60-300 FEI at 80 kV), EELS (Titan cubed G2 60-300 FEI at 80 kV), XPS (Thermo VG Scientific Sigma Probe equipped with monochromatic Al Kα-source), dispersive Raman spectra (LabRAM HR UV/vis/NIR-Horiba Jobin Yvon), XRD (D/MAX-2500, Rigaku with Cu Kα radiations). Nitrogen adsorption-desorption isotherms at 77 K were measured using surface area analyzer (BELSORP-max) to calculate BET surface area and pore size distribution. NLDFT model was used to measure the pore size distribution of the samples by assuming slit-like pore geometry.

Compression, electrical and electrochemical measurements

Compressive characteristics of different cylindrical aerogels were measured using a table-top universal testing machine (AGS-X, Shimadzu Corp.) with a crosshead speed of 2 mm min^{-1}. Electrical conductivity of the cylindrical uncompressed aerogels was determined by a two-electrode method (Keithley, DMM 7510 digital multimeter) using two metal wires as current collectors. In order to make proper electrical connection between conductive Cu foil and aerogels, each end of the aerogels was affixed to Cu foil with a thin layer of silver paste. Electrical conductivity of the compressed aerogel films was measured by a four-point probe method (Keithley 2400 Source meter). Two types of electrodes were prepared for electrochemical measurements; one was the flat thin electrode of individual NS-HGA, NS-GA and pristine GA from cutting and pressing and the other was the direct use of cubic aerogel of NS-HGA to study the electrochemical performance under various compressions. The electrochemical performances of the aforementioned electrodes (on the basis of the area of electrodes dipped in the solution) were investigated in a conventional three-electrode cell using a multichannel potentiostat/galvanostat analyzer (VersaStat 3, Princeton Applied Research), with Pt rod as counter electrode, Ag/AgCl (in saturated KCl) as reference electrode in 5 M LiCl aqueous solution. Electrochemical impedance spectroscopy (EIS) over a frequency range from 0.01 Hz to 100 KHz by applying sinusoidal signal of 10 mV amplitude was measured for aerogel electrodes in the solid-state.

The areal capacitances of the compressed aerogel electrodes in three-electrode system and areal or volumetric capacitances of the SRSS devices in two-electrode system were calculated from their CV curves and GCD curves according to the following equations, respectively:

$$\boldsymbol{C} = \frac{\mathbf{1}}{\boldsymbol{v}\,\boldsymbol{S}\Delta\boldsymbol{V}} \int_{V_1}^{V_2} \boldsymbol{I}\boldsymbol{d}\boldsymbol{V} \quad (1)$$

$$\boldsymbol{C_{ar}} = \frac{\boldsymbol{I}\boldsymbol{d}\boldsymbol{t}}{\boldsymbol{S}\boldsymbol{d}\boldsymbol{V}} \quad (2)$$

$$\boldsymbol{C_{Vol}} = \frac{\boldsymbol{I}\boldsymbol{d}\boldsymbol{t}}{\forall \boldsymbol{d}\boldsymbol{V}} \quad (3)$$

where C is the areal capacitance ($mFcm^{-2}$) from CV curves, C_{ar} is the areal capacitance ($mF\ cm^{-2}$) from GCD curves, C_{Vol} is the volumetric capacitance ($mF\ cm^{-3}$) from GCD curves, I is the current (mA), v is the scan rate ($mV\ s^{-1}$), S is the area of the single electrodes dipped in the solution or the total area of two electrodes (cm^2), t is the discharge time (s), V is the voltage (V), ∀ is the volume of the SRSS device (cm^3), and ΔV is the potential window (V).

The areal energy density E_{ar} (μWh cm^{-2}) or volumetric energy density E_{Vol} (μWh cm^{-3}) and areal power density P_{ar} (μW cm^{-2}) or volumetric power density P_{Vol} (μW cm^{-3}) of the device were calculated using the following equations:

$$\boldsymbol{E_{ar}} = \frac{\boldsymbol{C_{ar}}\Delta\boldsymbol{V^2}}{\mathbf{2\times 3.6}} \quad (4)$$

$$\boldsymbol{E_{Vol}} = \frac{\boldsymbol{C_{Vol}}\Delta\boldsymbol{V^2}}{\mathbf{2\times 3.6}} \quad (5)$$

$$P_{ar\ (or\ Vol)} = \frac{3600 \times E_{ar\ (or\ Vol)}}{\Delta t} \quad (6)$$

Coulombic efficiency (η) was calculated from the GCD curves of the devices using the following equations:

$$\eta = \frac{\Delta t_d}{\Delta t_c} \times 100\% \quad (7)$$

where Δt_d and Δt_c are discharging and charging time of the GCD curves, respectively.

Plausible mechanism for the formation of holey graphene sheets followed by heteroatom co-doping in NS-HGA

The plausible mechanism for the formation of holey graphene sheets followed by heteroatom co-doping is presented in Fig. S1. The formation of holey graphene sheets with generation of oxygen containing groups (lactones, anhydrides, carboxylic acids) at the defect sites proceeded through oxidative etching process of GO sheets by adding controlled amount of H_2O_2. Such generation of oxygen containing groups facilitated to interact with more amount of cysteamine (not only as N and S source but also as spacer arms between adjacent holey graphene sheets to hinder restacking of themselves) for bridging the holey graphene sheets under hydrothermal process to develop cysteamine functionalized holey graphene aerogel. After thermal annealing under Ar atmosphere, N and S co-doping took place in each holey graphene sheets of aerogels through the decomposition of 2° and 3° amine and thiol linkage by releasing high-fraction of volatile gases (like NH_3, H_2S, CO_2, etc.) provide finally graphitic N, pyridinic N, pyrrolic N, C-S-C, C=S and S-O or S=O.

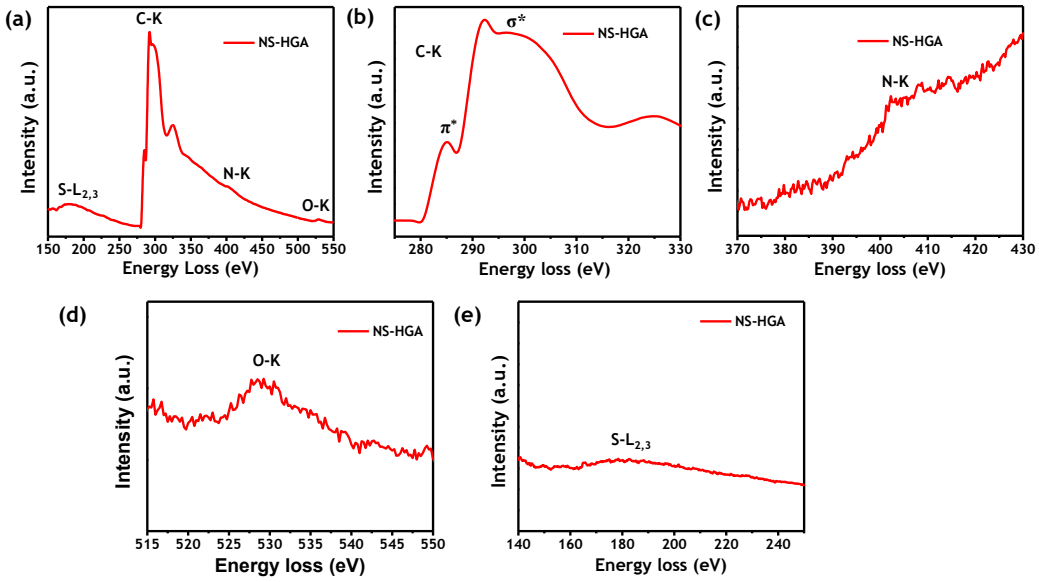

Fig. S2 a-e) Electron energy-loss spectroscopy (EELS) of each elements and their overlapped EELS spectroscopy for NS-HGA.

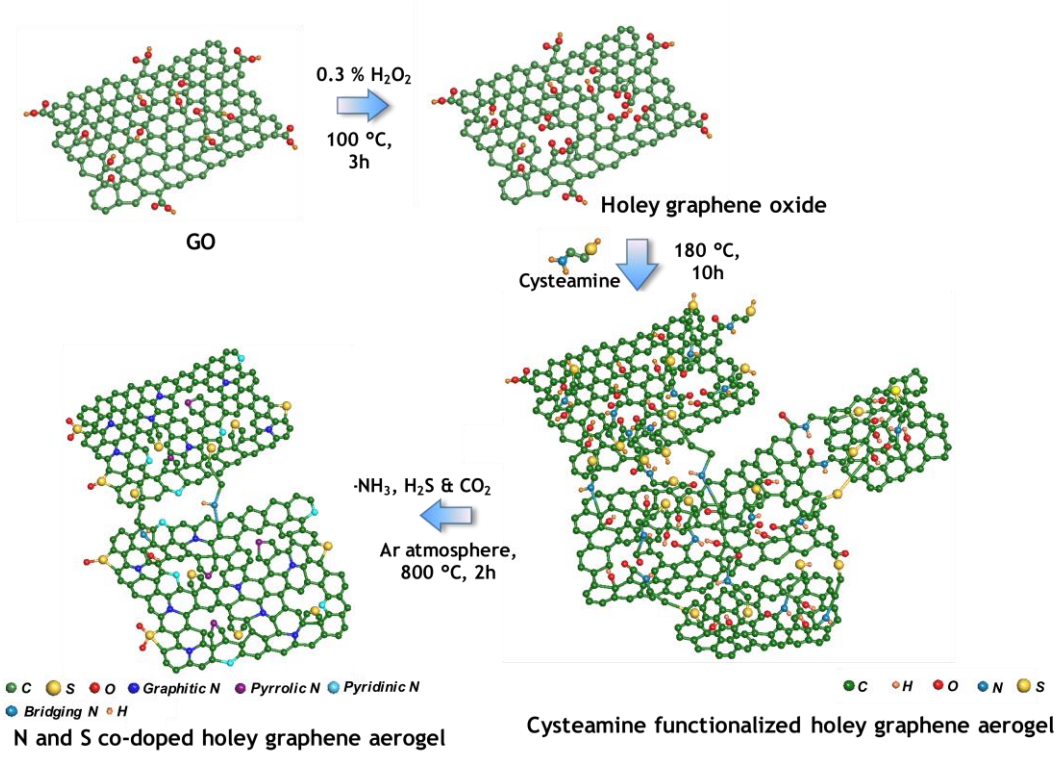

Fig. S1 Plausible mechanism for formation of holey graphene sheets followed by heteroatom co-doping in NS-HGA.

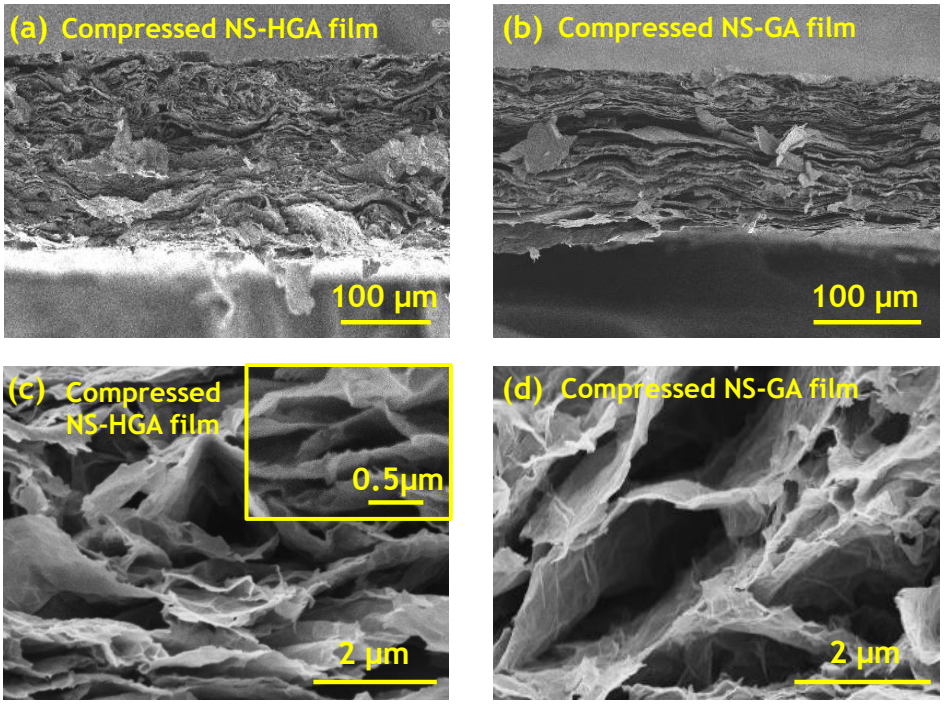

Fig. S3 Morphological analyses of compressed (ε > 85%) graphene aerogels: Cross-sectional FESEM low-magnification images of a) NS-HGA, b) NS-GA, high-magnification images of c) NS-HGA and d) NS-GA.

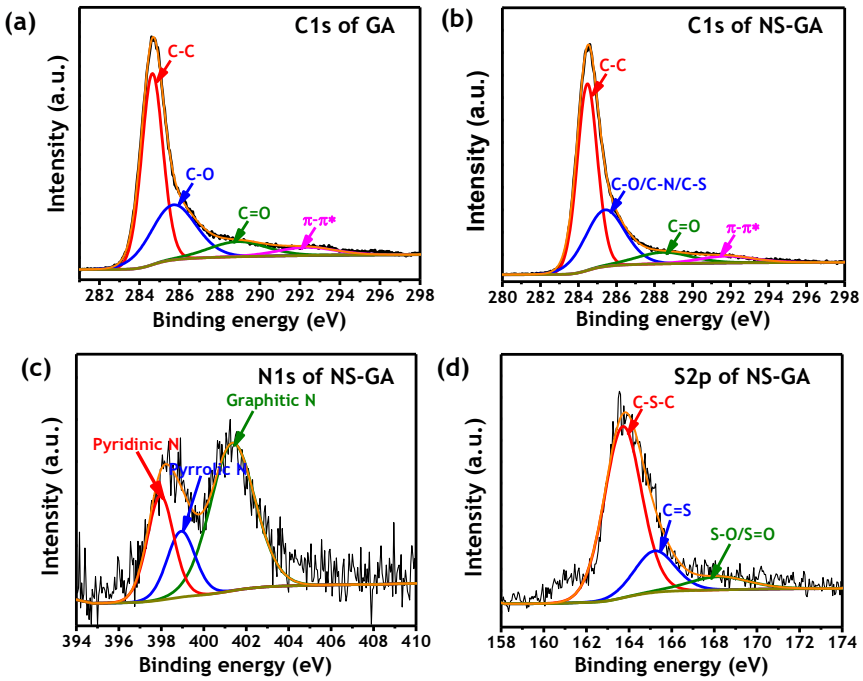

Fig. S4 High-resolution XPS spectra of a) C1s of pristine GA, b) C1s of NS-GA, c) N1s of NS-GA and d) S2p of NS-GA.

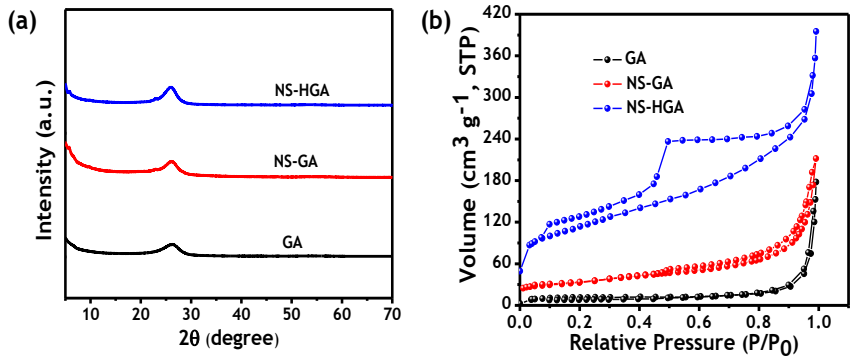

Fig. S5 Structural characterization of different graphene aerogels: a) XRD patterns and b) N_2 adsorption/desorption isotherms of NS-HGA, NS-GA and pristine GA.

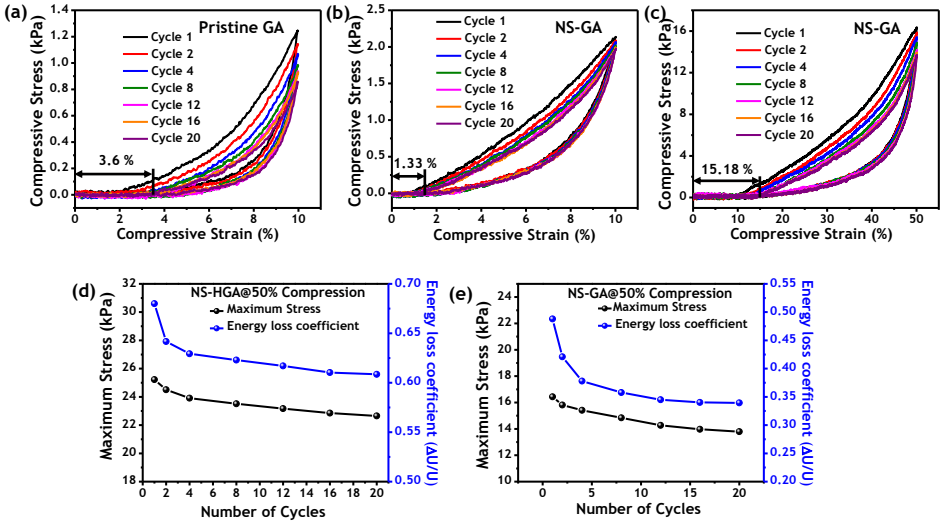

Fig. S6 Compressive properties of different graphene aerogels: Compressive stress-strain curves for 20 loading-unloading cycles of a) pristine GA at a maximum strain of 10%, NS-GA at a maximum strain of b) 10% and c) 50%. Maximum stress and energy loss coefficient for 20 compression cycles for d) NS-HGA and e) NS-GA derived from their corresponding compressive stress-strain curves under 50% strain.

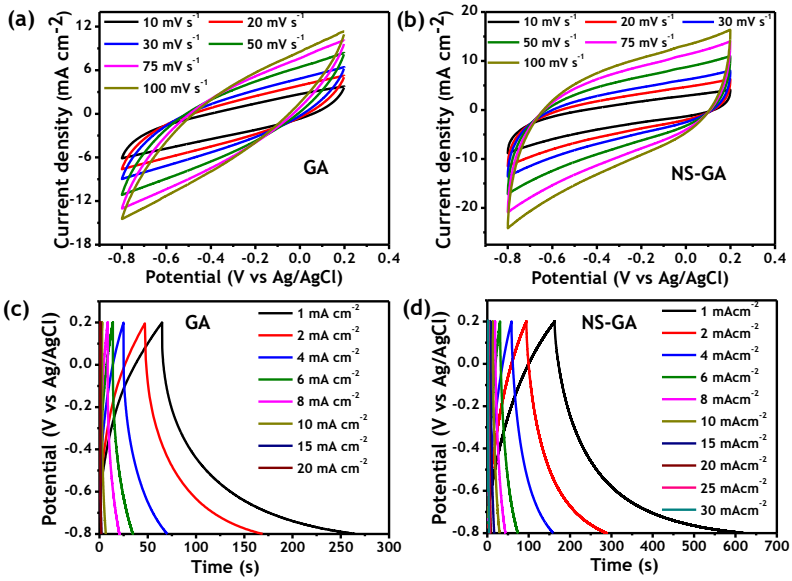

Fig. S7 Electrochemical performances of different graphene aerogels in 5 M LiCl: CV curves at various scan rates of a) pristine GA and b) NS-GA. GCD curves at various current densities of c) pristine GA and d) NS-GA.

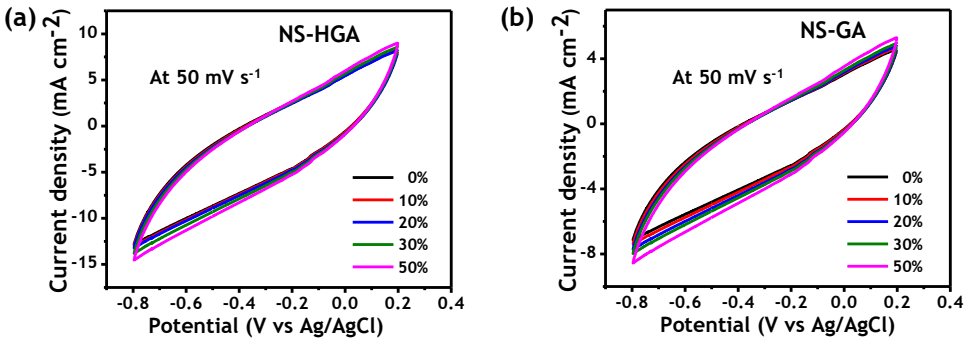

Fig. S8 CV curves of a) NS-HGA and b) NS-GA with different compressions at 50 mV s^{-1} collected in 5 M LiCl.

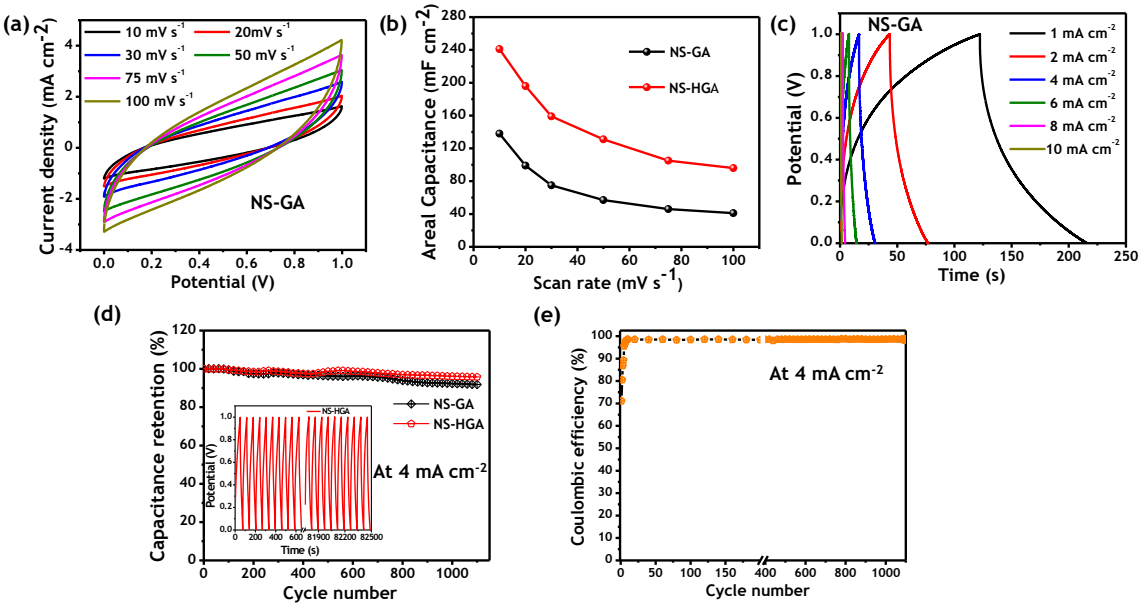

Fig. S9 Structurally resilient solid-state supercapacitors based on compressed NS-HGA and NS-GA films; a) CV curves of NS-GA:SRSS at various scan rates. b) Variation of areal capacitances with scan rates for NS-HGA:SRSS and NS-GA:SRSS. c) GCD curves of NS-GA:SRSS at different current densities. d) Cycling performance of NS-HGA:SRSS and NS-GA:SRSS at 4 mA cm^{-2}. Inset: The corresponding first 10 and last 10 GCD curves for NS-HGA:SRSS. e) Coulombic efficiency with cycle number during cycling performance at 4 mA cm^{-2}.

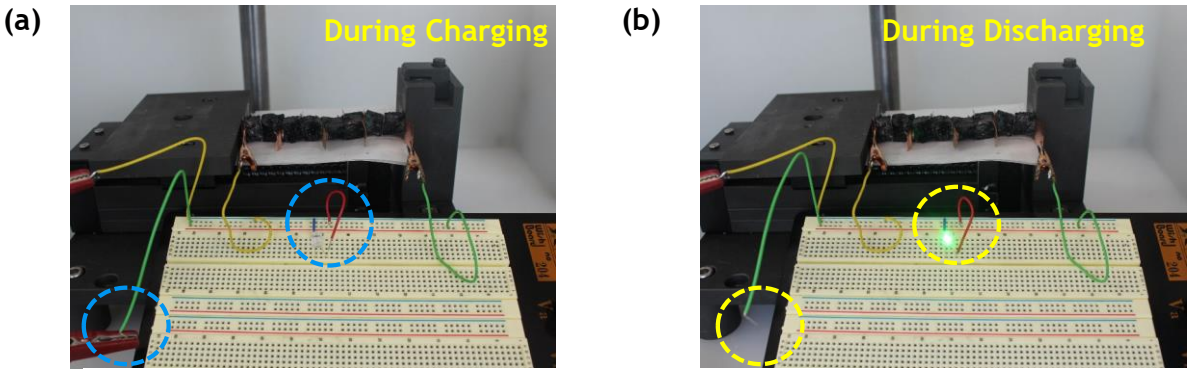

Fig. S10 Real-time optical images of the resultant tandem solid-state devices based on four supercapacitors of NS-HGA connected together in series during a) charging (indicating by blue circles) and b) discharging (indicating by yellow circles) showing the illumination of bright green LED. The green wire indicates for positive electrode and yellow wire indicates for negative electrode.

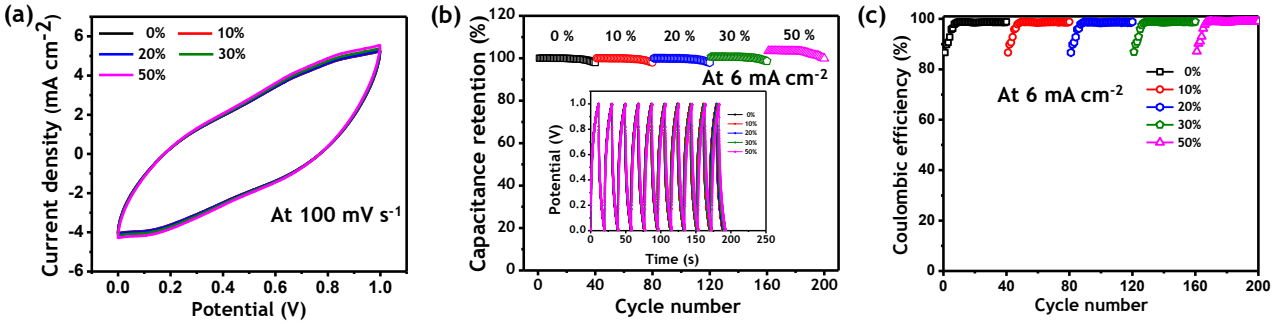

Fig. S11 Electrochemical responses of compressible SRSS device based on NS-HGA under compressive loads; a) CV curves under different compressions at 100 mV s^{-1}. b) Cycling performance under different compressions for 200 cycles at 6 mA cm^{-2}. Inset: The corresponding first 10 GCD curves with different compressions. c) Coulombic efficiency (η) with cycle number under different compressions during cycling performance at 6 mA cm^{-2}.

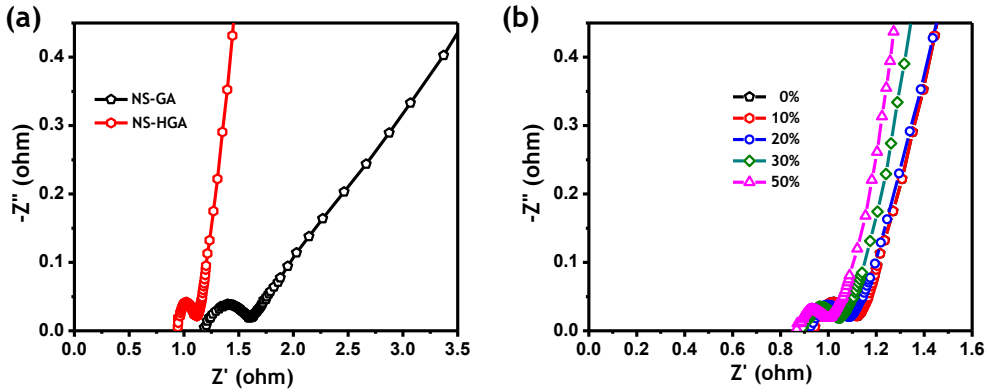

Fig. S12 Nyquist plots using PVA/LiCl gel electrolyte in solid-state (two-electrode system) of a) NS-GA and NS-HGA and b) NS-HGA under different compressions (ε = 10% to ε = 50%) over frequency range from 0.01 Hz to 100 kHz.

Table S1. Carbon, oxygen, nitrogen, and sulfur contents of pristine GA, NS-GA and NS-HGA.

Sample	Content (%)						
	C	O	N	S	C/O	C/N	C/S
GA	91.03	8.97	-	-	10.15		
NS-GA	93.05	3.4	1.92	1.63	27.36	48.46	57.08
NS-HGA	90.64	4.38	3.11	1.87	20.69	29.14	48.47

Table S2. Electrical conductivity by two-probe method of different graphene aerogels under zero compression.

Sample	Electrical conductivity (S m^{-1})
GA	2.50
NS-GA	12.43
NS-HGA	21.66

References

1 W. S. Hummers and R. E. Offeman, *J. Am. Chem. Soc.,* 1958, 80, 1339-1339.